



**HAL**  
open science

## Reactivity and a Charge-Transfer Model Analysis in Aminopolycarboxylic–Metal Complexes

Nawel Redjem, Salima Lakehal, Aicha Lakehal, Christophe Morell, Lynda  
Merzoud, Henry Chermette

► **To cite this version:**

Nawel Redjem, Salima Lakehal, Aicha Lakehal, Christophe Morell, Lynda Merzoud, et al.. Reactivity and a Charge-Transfer Model Analysis in Aminopolycarboxylic–Metal Complexes. *Inorganic Chemistry*, 2022, 61 (11), pp.4673-4680. 10.1021/acs.inorgchem.1c03860 . hal-04279835

**HAL Id: hal-04279835**

**<https://hal.science/hal-04279835>**

Submitted on 10 Nov 2023

**HAL** is a multi-disciplinary open access archive for the deposit and dissemination of scientific research documents, whether they are published or not. The documents may come from teaching and research institutions in France or abroad, or from public or private research centers.

L'archive ouverte pluridisciplinaire **HAL**, est destinée au dépôt et à la diffusion de documents scientifiques de niveau recherche, publiés ou non, émanant des établissements d'enseignement et de recherche français ou étrangers, des laboratoires publics ou privés.

# Reactivity and a charge transfer model analysis in aminopolycarboxylic-metal complexes

Nawel Redjem<sup>1</sup>, Salima Lakehal<sup>2,3,\*</sup>, Aicha Lakehal<sup>4</sup>, Christophe Morell<sup>5</sup>, Lynda Merzoud<sup>5</sup>, Henry Chermette<sup>5,\*</sup>

<sup>1</sup>Laboratoire de Chimie Appliquée et Technologie des Matériaux, Université Larbi Ben M'hidi Oum el Bouaghi, 04000 Oum El Bouaghi, Algeria

<sup>2</sup>Laboratoire de Chimie des Matériaux et des Vivants : Activité & Réactivité, Université Batna1, 05000 Batna, Algérie

<sup>3</sup>Institut des sciences de la terre et de l'univers, Université de Batna2, 05001 Batna, Algérie

<sup>4</sup> Faculté des sciences techniques, Université de Batna2, 05000 Batna, Algérie

<sup>5</sup> Université de Lyon, Université Claude Bernard Lyon 1, UMR CNRS 5280, Institut des Sciences Analytiques, 69622 Villeurbanne Cedex, France

Supporting Information Placeholder

---

**ABSTRACT:** In the present work, we have calculated several DFT reactivity descriptors for the aminopoly carboxylates acids (APCs) at B3LYP/6311++G (d,p) levels of theory aiming to analyze its reactivity. Reactivity descriptors such as ionization energy, molecular hardness, electrophilicity, and condensed Fukui function local indices have been determined to predict the reactivity of APCs. The influence of the solvent was taken into account employing the CPCM model. The results indicate that the solvation slightly modifies the tendency of the reactivity of the APCs studied. On the other hand, we applied a global and local charge transfer partitioning model, which introduces two charge transfer channels (one for accepting electrons (electrophilic) and another for donating one (nucleophilic)), to the complexation reaction of a set of APC acids with transition metals (the Mn, Co and Ni target enlarged by Fe, Cu and Zn). The correlation between the charges obtained for the interaction between APC acids and transition metals stability constants provides support for their interpretation as measures of the electrophilicity and nucleophilicity of a chemical species, and, at the same time, allows one to describe the donation and back-donation processes in terms of the density functional theory of chemical reactivity. Also, the application of dual descriptors for this acids provides valuable information concerning the atoms in the reactants playing the most important roles in the reaction, and thus, helping to improve our understanding of the reaction under study.

---

## 1. INTRODUCTION

The contamination by heavy metals has been a serious problem in the last decades. The aminopolycarboxylates acids (APCs) have been widely used as ligands to capture the heavy metals. Therefore, the APC structures are also known for their good possibilities of heavy atom recovery. The chelation and dechelation of APCs complexes have been proposed as a novel green approach for heavy metal capture. However, the reactivity of the heavy metals with the APCs complexes is still the subject of several investigations<sup>1-5</sup>.

Conceptual density functional theory is widely applied in various fields for understanding chemical reaction using the isolated properties of reactants<sup>6-16</sup>. It has been successfully exploited to unravel chemical reactivity and sites selectivity. To explain the chemical reaction without knowing a detailed knowledge of the reaction path, conceptual density functional theory uses global and local chemical

descriptors<sup>17-19</sup> which contain reactivity information of the whole system.

Among chemical descriptors the most common ones involving global reactivity information are the chemical potential  $\mu$ , the hardness  $\eta$  and global softness  $S^{20,21}$ . Another important local descriptors are the Fukui functions  $f(r)^{10}$ , dual descriptors<sup>22,23</sup> and the local softness  $s(r)^{24}$ . These and other chemical reactivity indexes have been reviewed in the literature<sup>18,25-28</sup>.

In the association reaction  $X + Y \rightarrow XY$ , one can show that the change in the energy involved can easily be expressed in terms of the electronegativities and hardnesses of the reacting species, by using the Parr and Pearson (PP) model<sup>6,29</sup>

Aiming to determine the charge-transfer mechanism, electrophilic or nucleophilic, prevailing in an association chemical reaction, Orozco-Valencia et al. presented recently a partitioning scheme for the number

of electrons exchanged in a reaction considering that both species accept and donate charge<sup>30,31</sup>.

The main objective of this study is to explore the reactivity of the APC acids with respect to the complexation of some transition metals, namely Ni, Co and Mn, as presented in Figure 1.

Therefore, we carried out our study on three steps. The first one is the analysis of APCs reactivity by calculating different reactivity indices to determine which atoms in all of these acids plays the most important role in the reactions. In a second step, the charge transfer partition is calculated based on the global PP model, aiming to establish a correlation between the charge quantities transferred and the equilibrium constants. In the third step, the molecular orbitals of eight stable structures of EDTA are analyzed to understand the behaviour of APCs in these reactions. Besides, a natural population analysis (NBO) is carried out on all the nickel complexes.

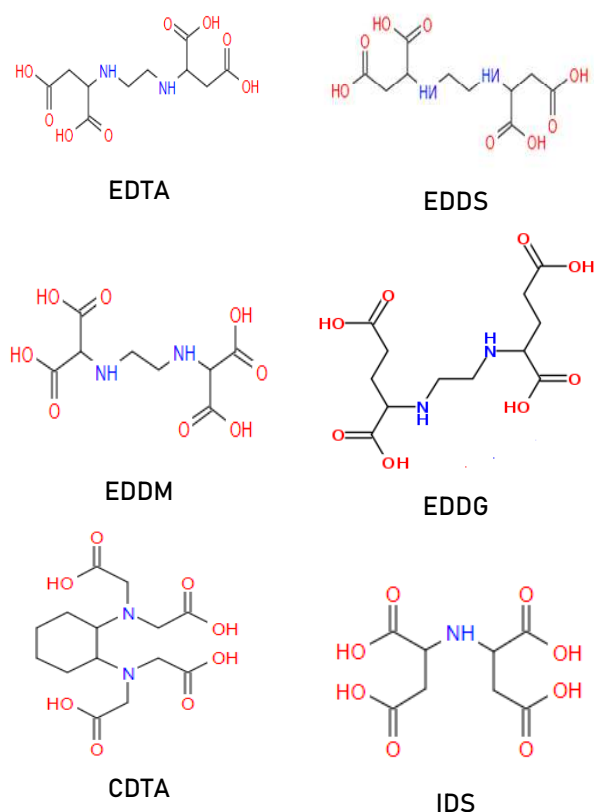


**Fig. 1** the different aminopolycarboxylic acids with four carboxylic functions

The paper is organized as follows: after the description of computational methodology, we will study in the first part the relative reactivity prediction, the

second part will be devoted to the dual descriptor and the Molecular Electrostatic Potentials, the last part will focus in the charge transfer between metal and ligand. The natural bond orbitals (NBO) analyses is also carried out and discussed. The paper ends with some concluding remarks

## 2. COMPUTATIONAL METHOD

All DFT calculations reported in this work were done employing the hybrid B3LYP functional<sup>32-34</sup> and the 6-311++G (d, p) basis set<sup>35,36</sup>. For transition metals, we use the LANL2DZ basis set. This standard and widely used functional is known to deliver rather good structures of organometallic systems (see, e.g. ref. 37-39). A frequency analysis was done to confirm that all the stationary points located by the optimization procedure correspond to minima in the potential energy surface. Optimized APCs molecules in the gas phase were further re-optimized at the B3LYP/6311++G (d, p) level employing CPCM solvation model<sup>40,41</sup> in the aqueous medium. All the calculations reported here were performed with the Gaussian 09 package<sup>42</sup>, visualized with the Gauss View<sup>43</sup> and Gabedit packages<sup>44</sup>. Electronic chemical potential and chemical hardness and softness were calculated from the frontier molecular orbital (FMO) eigenvalues. The natural bond orbital (NBO) calculations have been performed for each reactant using the NBO 3 program<sup>45</sup> interfaced with Gaussian 09<sup>42</sup>.

Global reactivity descriptors indices such as electronegativity, electronic chemical potential ( $\mu$ ) (which is equal to the negative of the electronegativity), hardness ( $\eta$ ), electrophilicity index ( $\omega$ )<sup>12,18,25-28,46</sup>, are calculated according to Koopmans' theorem as follow:

$$\mu \approx -\frac{1}{2}(I + A) \quad (1)$$

where  $I = -E_{\text{HOMO}}$  and  $A = -E_{\text{LUMO}}$

$$\mu \approx \frac{\epsilon_{\text{LUMO}} + \epsilon_{\text{HOMO}}}{2} \quad (2)$$

$$\eta \approx I - A \quad (3)$$

$$\eta \approx \epsilon_{\text{LUMO}} - \epsilon_{\text{HOMO}} \quad (4)$$

The global softness ( $S$ ) is defined as the reciprocal hardness as follow:

$$S = \frac{1}{\eta} \quad (5)$$

The absolute electronegativity ( $\chi$ ) is defined as<sup>20</sup>

$$\chi = -\mu \quad (6)$$

The nucleophilicity index<sup>47</sup> is calculated referred to tetracyanoethylene (TCE) is given by:

$$N_u = \varepsilon_{\text{HOMO}(\text{Nuc})} - \varepsilon_{\text{HOMO}(\text{TCE})} \quad (7)$$

where:  $\varepsilon_{\text{HOMO}(\text{TCE})} = -9.367\text{eV}$ <sup>47</sup> (In our computational conditions (same functional, same basis set, same solvent), one gets  $\varepsilon_{\text{HOMO}(\text{TCE})} = -9.303\text{ eV}$ ). The tiny shift does not affect the trends, evidently.

The global electrophilicity index  $\omega$  was introduced by Parr<sup>8,18,25</sup> and it is calculated using the electronic chemical potential  $\mu$  and the absolute hardness  $\eta$ :

$$\omega = \frac{\mu^2}{2\eta} \approx \frac{(I + A)^2}{8(I - A)} \quad (8)$$

Accordingly,  $\omega$  measures the ability of a species to accept electrons. Thus, low values of  $\omega$  indicate a good nucleophile while high values characterize good electrophiles.

### Relative reactivity prediction

The relative reactivity of substitutions has been rationalized using the global nucleophile index proposed by Domingo et al.<sup>47</sup> defined according to equa-

tion 7. As is well known, the HOMO and LUMO frontier molecular orbitals provide understanding in the efficiency in the interaction between chemical reactants: A high value of the quantum chemical descriptor  $\varepsilon_{\text{HOMO}}$  favors the molecule to electron donation, whereas a low value of  $\varepsilon_{\text{LUMO}}$  favors the electron capture by the molecule. The hardness helps us to characterize the chemical reactivity and the kinetic stability of the molecular product.

From Table 1, the results reveal that all of the acids have strong gap values, which indicates good stability. On the other hand, by examining the values of global nucleophilicity index, we note that the CDTA ligand has the greatest nucleophilic index ( $N_u = 3.727, 3.545$  in gas, solvent phases, respectively) compared to the other ligands.

The analysis of HOMO energy, which acts as an electron donor<sup>48</sup>, indicates a tendency for the molecule to donate an electron to the appropriate metal as an electron acceptor. Let us recall that a good nucleophile has high chemical potential and a high value of HOMO energy, and has low electrophilicity index  $\omega$ . This tendency is:

CDTA > EDTA > EDDM > EDDS > EDDG > IDS

Table 1: Calculated quantum chemical parameters and global reactivity descriptors of the studied APCs ligands (italic values for solvated species) in eV. (eV<sup>-1</sup> for S)

Ligand	$\varepsilon_{\text{HOMO}}$	$\varepsilon_{\text{LUMO}}$	Nu	$\mu$	X	$\eta$	S	$\omega$	$\Delta N_{\text{max}}$
CDTA	-5.641/-5.823	-0.979/-1.017	3.727/3.545	-3.310/-3.420	3.310/3.420	4.662/4.805	0.214/0.208	1.174/1.217	0.710/0.712
EDTA	-6.040/-6.548	-0.572/-0.646	3.328/2.82 <i>C</i>	-3.306/-3.597	3.306/3.597	5.468/5.902	0.183/0.169	0.999/1.100	0.604/0.609
EDDS	-6.772/-6.952	-0.859/-0.769	2.592/2.416	-3.815/-3.861	3.815/3.861	5.913/6.182	0.169/0.162	1.231/1.205	0.645/0.624
EDDM	-6.773/-6.905	-0.927/-0.999	2.595/2.462	-3.850/-3.952	3.850/3.952	5.846/5.906	0.171/0.169	1.268/1.322	0.658/0.669
EDDG	-7.061/-6.736	-0.953/-0.674	2.306/2.632	-4.007/-3.705	4.007/3.705	6.108/6.062	0.164/0.165	1.314/1.132	0.656/0.611
IDS	-7.126/-6.871	-0.993/-0.894	2.242/2.497	-4.060/-3.882	4.059/3.882	6.133/5.977	0.163/0.167	1.343/1.261	0.662/0.649

It can be observed from Table 1 that the global hardness  $\eta$  is slightly modified when the solvent is taken into account with respect to the gas phase. One of the reasons is that a polar solvent, such as water, could stabilize the charged species with respect to the gas phase, therefore modifying the value of  $\eta$  without having a direct implication on the reactivity of the APCs.

### 3. DUAL DESCRIPTOR

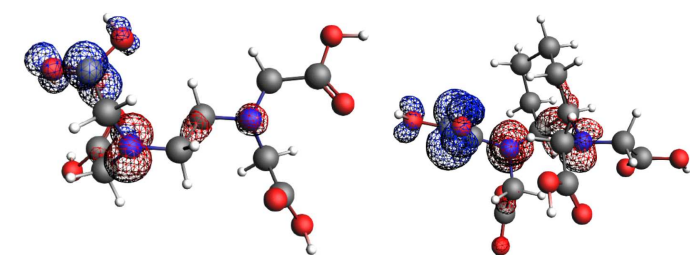
The dual descriptor (DD)  $\Delta f(r)$ , introduced by Morell<sup>22,23</sup> measures how the absolute hardness changes with an external potential change. Typically, this occurs when reactants approach each other during a bimolecular reaction. The DD can also be defined as the second derivative of the electron density with respect to the number of electrons, and

ored in red, whereas positive ( $\Delta f(r) > 0$ ) regions are blue. As expected, the negative regions of the DD are located on the nitrogen atoms, indicating that any electrophilic attack would take place on the nitrogen lone pairs. This is expected because the HOMO (and HOMO-1) should be located on the lone pairs of the nitrogen(s). We will discuss this point below.

#### 4. MOLECULAR ELECTROSTATIC POTENTIALS (MEP)

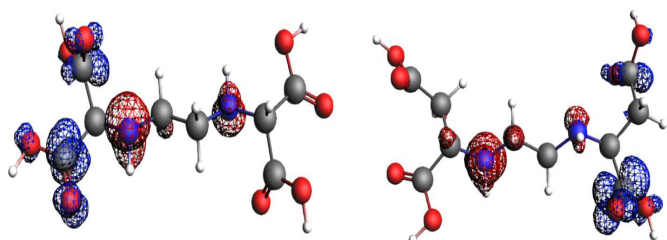
MEPs are also used to investigate the chemical reactivity of a molecule. Former works on the application of MEP to chemical facts<sup>49-52</sup> highlighted the possibilities of MEP in the interpretation of reactivity. This is especially important for the identification of the reactive sites of nucleophilic or electrophilic attack.

The MEP surface shows the charges distribution in the different acids. The electrostatic potential increases in the following order: red < yellow < green < blue. The negative regions are red and the blue ones indicate positive regions. The resulting overall MEP of the different APCs (Figure 3) shows that the red regions are located on the oxygen atoms (C=O) indicating that those oxygen atoms will be the preferred sites for electrophilic attack.



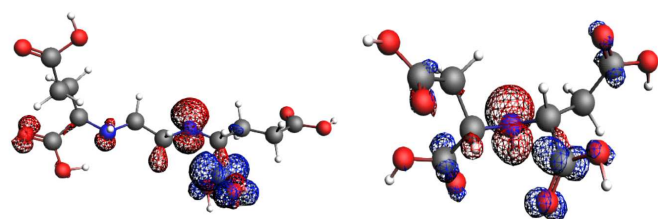
EDTA

CDTA



EDDM

EDDS



EDDG

IDS

**Figure 2.** Dual descriptors of the 6 APCs (isocontours = 0.005au)

it can be calculated as the difference between the electrophile and nucleophile Fukui functions:

$$\Delta f(\mathbf{r}) = f^+(\mathbf{r}) - f^-(\mathbf{r}) \quad (9)$$

Accordingly, where  $\Delta f(\mathbf{r}) > 0$ , nucleophilic attack is favored rather than electrophilic attack, whereas if  $\Delta f(\mathbf{r}) < 0$ , point  $\mathbf{r}$  favors electrophilic attack. Consequently, positive values of  $\Delta f(\mathbf{r})$  point out electrophilic regions within a molecular topology, whereas negative values of  $\Delta f(\mathbf{r})$  highlight nucleophilic regions. Maps of the dual descriptors for each APCs acids are shown in Fig. 2. Negative ( $\Delta f(\mathbf{r}) < 0$ ) regions are col-

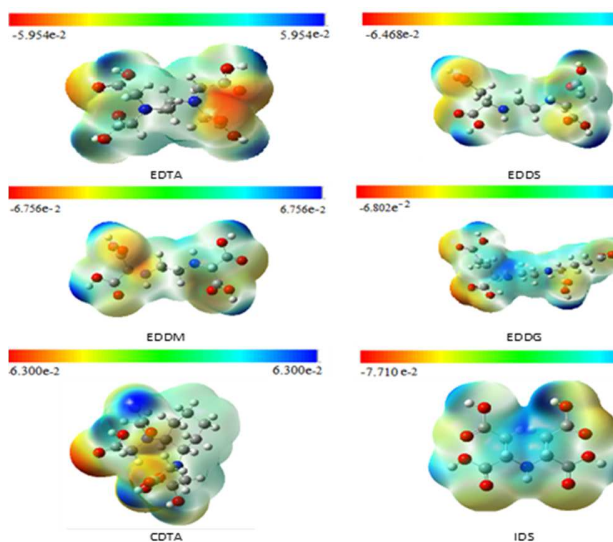


**Fig. 3.** Electrostatic potentials mapped on the electron density surface of the 6 APCs

**Figure 3.** Electrostatic potentials mapped on the electron density surface of the 6 APCs

## 5. MO OCCUPATION

The MOs diagrams show clearly that the HOMO and HOMO-1 (for the five chelating ligands holding two nitrogens) are typically the orbitals holding the lone pairs of the nitrogen(s), as expected. Since several stable conformations can be optimized, it is interesting to see, among these conformations, if these lone

pairs are identically occupied by the two orbitals or if the HOMO is more localised on a given nitrogen, whereas the HOMO-1 is in the majority localised on the other nitrogen. Table 2 reports the case of 8 different structures of EDTA for which we can observe that the energy gap between the HOMO and HOMO-1 is neither related to the stability of the structure, nor to a localisation/delocalisation on the nitrogens.

**Table 2:** The calculated energy gap for 8 different structures of EDTA (eV)

Structure number	Total Bonding Energy kcal/mol	"Gap" HOMO-HOMO-1	HOMO-1 $\pi$ N12	HOMO-1 $\pi$ N11	HOMO $\pi$ N12	HOMO $\pi$ N11	HOMO-1 eigenvalue	HOMO eigenvalue
1	-5040.48	0.282	0	56	61	2	-5.853	-5.571
2	-5041.89	0.791	51	13	7	46	-5.896	-5.105
3	-5041.97	0.518	38	23	22	38	-5.913	-5.395
4	-5042.84	0.709	53	8	9	49	-5.967	-5.258
5	-5043.41	0.349	23	34	36	24	-5.42	-5.071
6	-5044.96	0.515	4	50	60	4	-5.911	-5.396
7	-5045.29	0.549	12	46	47	12	-5.497	-4.948
8	-5047.93	0.582	10	49	43	12	-5.472	-4.890

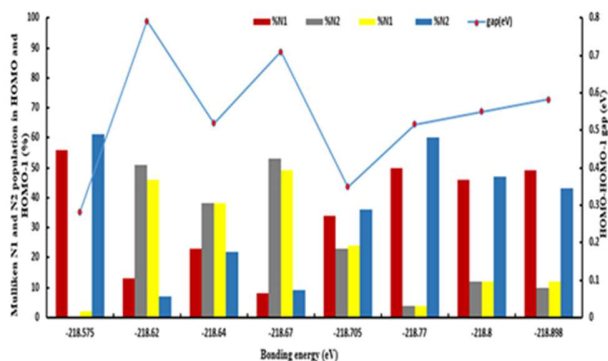


**Fig.4** HOMO-(HOMO-1) gap vs bonding energy among EDTA structures (kcal/mol). The N populations are that of HOMO (left) and HOMO-1 (right) for N1 and N2.

Surprisingly, there is no correlation between the stability of the conformer and the localization of the lone pairs on the two nitrogens. The localization, here measured by the Mulliken population of nitrogens in the HOMO and HOMO-1, is illustrated in Fig. 4. It clearly shows that the localization is maximum on a given nitrogen in the HOMO (and consequently maximum for the other nitrogen in the HOMO-1) for the most stable structure, but also for least stable ones (among the calculated structures). On the contrary, a few structures exhibit rather equally distributed lone pair electrons on the nitrogens among the

HOMO and HOMO-1. This large variation of the electron density among the different conformers lets expect an easy transformation towards more or less reactive conformations. The reactivity is probably *in fine* not necessarily related to the electronic properties of the most stable conformation of the ligand, but to one conformation exhibiting a more localized density on one nitrogen in the HOMO, leading to a starting complexation process. That will involve a geometry deformation relocating the density on the second nitrogen on the ligand fragment within the complex formation. A full analyse of the complexation process is out of the scope of the present work.

## 6. METAL-LIGAND NET CHARGE TRANSFER

In the density functional theory of chemical reactivity<sup>21,53</sup>, the charge transfer terms are related to the interaction energy as part of a covalent contribution. Orozco-Valencia et al.<sup>30,31</sup> have provided expressions for the transfer of charge  $\Delta N$  and of energy difference  $\Delta E$  which complete the formation of a complex between an acid A and a base B, namely:

$$\Delta E = \mu \Delta N + \frac{1}{2} \eta (\Delta N)^2 \quad (10)$$

Considering the interaction between two systems X and Y, and analyzing the process of charge transfer occurring between these two species, the charge

transfer between X and Y is given by the expression below:

$$\Delta N_X = N_X^{Ele} + N_X^{Nuc} \quad (11)$$

where  $N_X^{Ele}$  is the electrophilic component, representing the charge transferred in the electrophilic channel of reactant X, which means that X is accepting electrons (it must take positive value).  $N_X^{Nuc}$  is the nucleophilic component, which means that  $N_X^{Nuc}$  is the charge transferred through the nucleophilic channel of X, X being then donating electrons (it must be negative). There are similar equations for reactant Y where the roles are inverted in accordance with the charge conservation. In general, when the two reacting systems X and Y are neutral, the directions of charge transfer agree with the chemical potential differences. The expressions to calculate the amount of electrons transferred in these two channels are:

$$\Delta N_X^{Ele} = \frac{I_X - A_Y}{2(\eta_X + \eta_Y)} = -\Delta N_Y^{Nuc} \quad (12)$$

$$\Delta N_X^{Nuc} = \frac{A_X - I_Y}{2(\eta_X + \eta_Y)} = -\Delta N_Y^{Ele} \quad (13)$$

When the charge transfer increases, the interaction between the metal and the ligand is stronger<sup>36</sup>. According to the expressions 12 and 13, one can determine the back-donation and the donation between metals and APCs acids respectively. To apply these relationships to our systems, we need first to calculate the first vertical ionization potential I, and the vertical electron affinity A defined in eq(1), of the APCs acids, here considered as species X, and of the

**Table 3.** Ionization potential, electron affinity, chemical potential and hardness, in eV, for a set of APC ligands, and Mn, Co and Ni atoms.

	$I_Y$	$A_Y$	$\mu_Y$	$\eta_Y$
Mn	4.837	3.016	-3.926	1.821
Co	5.886	3.195	-4.540	2.691
Ni	4.884	3.242	-4.051	1.641
	$I_X$	$A_X$	$\mu_X$	$\eta_X$
CDTA	5.641	0.979	-3.310	4.662
EDTA	6.040	0.572	-3.306	5.468
EDDS	6.772	0.859	-3.815	5.913
EDDM	6.773	0.927	-3.850	5.846
EDDG	7.061	0.953	-4.007	6.108
IDS	7.126	0.993	-4.059	6.133

metal identified as species Y. The average chemical potential and the hardness  $\eta$ , of both species are collected in Table 3

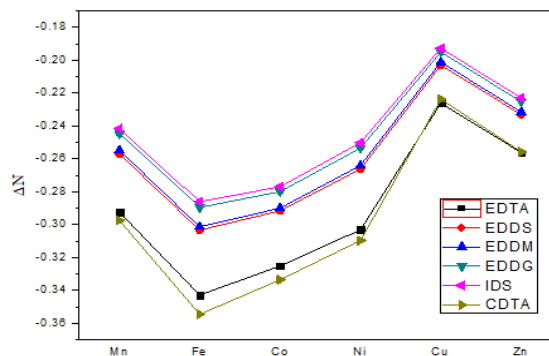


**Fig 5.** The variation of charge transfer according to metals

According to the results plotted in Fig. 5, it can be seen that the charge transfer for the same metal follows the descending order: IDS < EDDG < EDDM < EDDS < EDTA < CDTA. It is the same order as that we obtained for the HOMO eigenvalue and the electrophilicity index

We have gathered in Table 4 the calculated values of  $\Delta N_X$ ,  $\Delta N_X^{ele}$  and  $\Delta N_X^{nuc}$  obtained from Eq. (11), (12) and (13), respectively. We have also reported the experimental values of stability constants log K corresponding to the (APCs) metal complexes.

A negative sign of  $\Delta N_X^{nuc}$  indicates that charge is transferred from the ligand to the metal, while a positive value of  $\Delta N_X^{ele}$  indicates the opposite direction, the charge is transferred from the metal to the ligand. Their absolute values indicate the amount of charge transferred through the two channels.

**Table 4.** Net charge (Eq.11), electrophilic charge (Eq.12), nucleophilic charge (Eq.13), log K experimental values<sup>54</sup>

	Metal	$\Delta N_X^{ele}$	$\Delta N_X^{nuc}$	$\Delta N_X$	log K
EDTA	Mn	0.2074	-0.2925	-0.0851	13.9
	Co	0.1747	-0.3252	-0.1505	16.31
	Ni	0.1967	-0.3032	-0.1055	18.62
EDDS	Mn	0.2428	-0.2571	-0.0143	9.0
	Co	0.2082	-0.2917	-0.0835	14.02
	Ni	0.2336	-0.2663	-0.0327	16.7

	Mn	0.2450	-0.2549	-0.0099	8.45
EDDM	Co	0.2099	-0.2900	-0.0801	12.20
	Ni	0.2358	-0.2641	-0.0283	14.5
EDDG	Mn	0.2550	-0.2449	0.0101	6.74
	Co	0.2200	-0.2799	-0.0599	10.62
	Ni	0.2464	-0.2535	-0.0071	13.04
IDS	Mn	0.2583	-0.2416	0.0167	7.3
	Co	0.2227	-0.2770	-0.0543	10.5
	Ni	0.2497	-0.2502	-0.0005	12.2
CDTA	Mn	0.2024	-0.2975	-0.0951	17.5
	Co	0.1661	-0.3336	-0.1675	19.7
	Ni	0.1902	-0.3097	-0.1195	20.2

Therefore, the stronger electron-withdrawing ligands correspond to those with larger  $\Delta N_X^{ele}$ , and the stronger electron-donating groups correspond to those with larger absolute value of  $\Delta N_X^{nuc}$ .

Figure 6 shows the overall correlation between  $\Delta N_X^{nuc}$  and the log K values of metal complexes, using Eqs. (10), (11) and (12), one can show that:

$$\Delta N_X^{ele} = \frac{1}{2} \Delta N_X + \frac{1}{4} \quad (14)$$

and:

$$\Delta N_X^{nuc} = \frac{1}{2} \Delta N_X - \frac{1}{4} \quad (15)$$

This approach provides a tool for measuring the capacity of the electron donor or the nucleophilicity of, in this case the APC ligands with  $\Delta N_X^{nuc}$ , and the electron acceptor capacity or electrophilicity with  $\Delta N_X^{ele}$ , of Mn, Co and Ni. From calculated results in Table 4, a good linear correlation is found by plotting the equilibrium constants of the complexation reaction with the amount of electrons transferred through the nucleophilic channel (see Figure 6). The same correlation is found for the amounts of electrons transferred, as defined in equations 11 and 14<sup>30</sup>.

It is important to note that the electron acceptor-donor properties measured with  $\Delta N_A^{nuc}$  and  $\Delta N_A^{ele}$  clearly depend on the chemical nature of the APCs.

The APCs ligands have electron donor atoms, such as the four O atoms and two N atoms which have the greatest electrodonation capacity, so that they give more charge to Mn, Co and Ni.

These ligands can be arranged according to the absolute values of  $\Delta N_X^{nuc}$  sorting them in decreasing order of their nucleophilicity, one gets: CDTA > EDTA > EDDS > EDDM > EDDG > IDS, (and the opposite trend for the values of  $\Delta N_A^{ele}$ ). This is the order already found in Table 1.

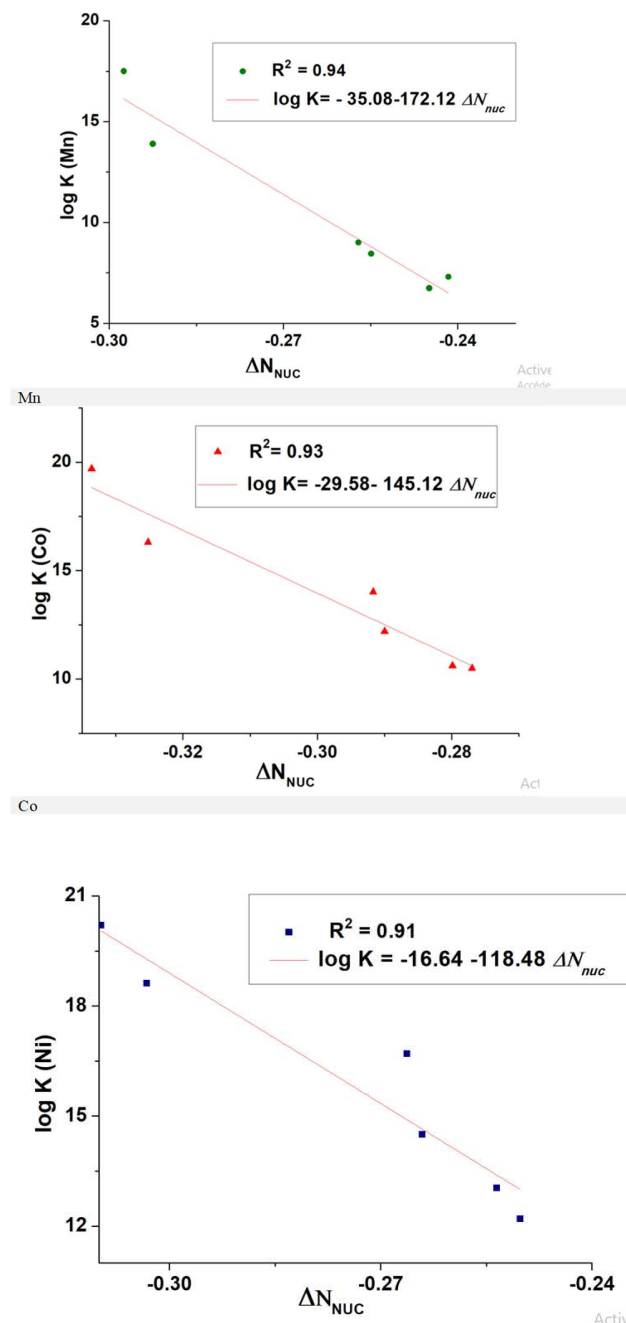


Fig. 6.. The equilibrium constant of the complexation reaction between APCs and Mn, Co, and Ni metals with the amount of electron transfer through the nucleophilic channel using values reported in Table 4.



## 5. NBO NICKEL COMPLEXES ANALYSIS

To highlight the donation and the back-donation of the metal–ligand, the NBO analysis is applied to the nickel complexes.

The second order perturbation analysis of the Fock matrix between the APCs and the transition metals are reported in Tables S.2-7 in SI. The NBO results show that, in those complexes, there is the interaction between  $\sigma$  (N-C),  $\sigma$  (C-O), LP (N) and LP (O) of the ligand with the nickel lone pair LP (Ni) and the weak interaction with  $Ry^*$  (Ni). However, a weak retrodonation from the Ni atom lone pairs to the ligand is noted except for the EDDS complex case, where a larger retrodonation is observed between  $LP^*$  (Ni) and  $Ry^*$  (C),  $\sigma^*$  (C-O) (see Table S.6. in SI). Therefore, the APCs complexes stabilization is due to the intramolecular charge transfer resulting from the N-C, C-O bonds as well as the nitrogen and oxygen atoms lone pairs of ligand to the nickel atom lone pairs.

## 6. CONCLUDING REMARKS

The results obtained in this work shed light on the driving forces in the complexation reactions of transition metals by APCs. MEPs and DD approaches allow one to clearly identify the atoms involved in the complexation reactions. The values of  $\Delta N_A^{nuc}$  and  $\Delta N_A^{ele}$  derived through the application of partitioning schemes provide information on the electrophilicity and nucleophilicity of the chemical species. Interestingly, we have found good correlations between these quantities and the complexation equilibrium constants for these metals.

Finally, the donation  $\sigma$  and the back-donation  $\pi$ , which is clearly framed in orbital language, can be reinterpreted in terms of charge transfer processes framed in the approach of the DFT for chemical reactivity<sup>26,55</sup>, and expressed in terms of important chemical concepts like chemical potential (electronegativity) and hardness of interacting species. The NBO results show that, the APCs complexes stabilization is due to the intramolecular charge transfer resulting from the sigma N-C, C-O bonds as well as the nitrogen and oxygen atoms lone pairs of ligand to the nickel atom lone pair. However, a weak retrodonation from the Ni atom lone pairs to the ligand is noted, the EDDS complex case excepted, where a more important retrodonation is observed between  $LP^*$  (Ni) and  $Ry^*$  (C),  $\sigma^*$  (C-O).

## ACRONYMS OF THE APCs

EDTA: Ethylenediaminetetraacetic acid  
EDDS: Ethylenediamine-N,N'-disuccinic acid  
EDDM: Ethylenediiminopropanedioic acid  
EDDG: Ethylenediamine-N,N'-diglutamic acid  
CDTA: Cyclohexanediaminetetraacetic acid  
IDS: Iminodisuccinic acid

## ASSOCIATED CONTENT

### Supporting Information

Table S1: structures and atom numbers

Tables S2-S7: NBO charges in the 6 complexes

## AUTHOR INFORMATION

\* To whom correspondence should be addressed.

E-mail: s.lakehal@univ-batna2.dz

E-mail: henry.chermette@univ-lyon1.fr

## ORCID:

Aicha Lakehal: a.lakhal@univ-batna2.dz, 0000-0001-6785-9643  
Nawel Redjem: nawelrjm@hotmail.fr 0000-0002-5411-7082  
Salima Lakehal: s.lakehal@univ-batna2.dz 0000-0003-1265-3597  
Christophe Morell: Christophe.Morell@univ-lyon1.fr, 0000-0002-6321-8723  
Lynda Merzoud: Lynda.Merzoud@isa-lyon.fr, 0000-0002-6003-8882  
Henry Chermette: henry.chermette@univ-lyon1.fr, 0000-0002-5890-7479

## Notes

Any additional relevant notes should be placed here.

## Acknowledgments:

The authors gratefully acknowledge the GENCI/CINES for HPC resources/computer time (Project cpt2130), as well as the PSMN of the ENS-Lyon for computing resources. N.R acknowledges HPC UFMC 1, Unité de Recherche de Chimie de l'Environnement et Moléculaire Structurale, CHEMS, Université Frères Mentouri Constantine 1, for support and computing resources.

## REFERENCES

- (1) Schmidt, C. K.; Fleig, M.; Sacher, F.; Brauch, H. J. Occurrence of Aminopolycarboxylates in the Aquatic Environment of Germany. *Environ. Pollut.* **2004**, *131* (1), 107–124. <https://doi.org/10.1016/j.envpol.2004.01.013>.

- (2) Kropacheva, T. N.; Antonova, A. S.; Kornev, V. I. The Influence of Aminopolycarboxylates on the Sorption of Copper (II) Cations by (Hydro)Oxides of Iron, Aluminum, and Manganese. *Eurasian Soil Sci.* **2016**, *49* (7), 765–772. <https://doi.org/10.1134/S1064229316070061>.
- (3) Królicka, A.; Zar, A.; Bobrowski, J. Application of Aminopolycarboxylic Complexes of V (IV) in Catalytic Adsorptive Stripping Voltammetry of Germanium. *Chemosensors.* **2022**, *10* (1), 1–20. <https://doi.org/10.3390/chemosensors10010036>.
- (4) Rahman, M. A.; Rahman, M. M.; Maki, T.; Hasegawa, H. The Significance of Biodegradable Methylglycinediacetic Acid (MGDA) for Iron and Arsenic Bioavailability and Uptake in Rice Plant. *Soil Sci. Plant Nutr.* **2012**, *58* (5), 627–636. <https://doi.org/10.1080/00380768.2012.717246>.
- (5) Lewis, K. M.; Greene, C. L.; Sattler, S. A.; Youn, B.; Xun, L.; Kang, C. The Structural Basis of the Binding of Various Aminopolycarboxylates by the Periplasmic Edta-Binding Protein Eppa from Chelatorans Sp. BNC1. *Int. J. Mol. Sci.* **2020**, *21* (11), 1–20. <https://doi.org/10.3390/ijms21113940>.
- (6) Pearson, R. G. Absolute Electronegativity and Hardness: Applications to Organic Chemistry. *J. Org. Chem.* **1989**, *54*, 1423–1430.
- (7) Pearson, R. G. Hard and Soft Acids and Bases—the Evolution of a Chemical Concept. *Coord. Chem. Rev.* **1990**, *100* (C), 403–425. [https://doi.org/10.1016/0010-8545\(90\)85016-L](https://doi.org/10.1016/0010-8545(90)85016-L).
- (8) Parr, R. G.; Szentpály, L. V.; Liu, S. Electrophilicity Index. *J. Am. Chem. Soc.* **1999**, *121* (9), 1922–1924. <https://doi.org/10.1021/ja983494x>.
- (9) Ayers, P. W.; Levy, M. Perspective on “Density Functional Approach to the Frontier-Electron Theory of Chemical Reactivity.” *Theor. Chem. Acc.* **2000**, *103* (3–4), 353–360. <https://doi.org/10.1007/s002149900093>.
- (10) Parr, R. G.; Yang, W. Density Functional Approach to the Frontier-Electron Theory of Chemical Reactivity. *J. Am. Chem. Soc.* **1984**, *106*, 4049–4050.
- (11) Ayers, P. W.; Parr, R. G. Variational Principles for Describing Chemical Reactions. Reactivity Indices Based on the External Potential. *J. Am. Chem. Soc.* **2001**, *123* (9), 2007–2017. <https://doi.org/10.1021/ja002966g>.
- (12) Ayers, P. W.; Anderson, J. S. M.; Bartolotti, L. J. Perturbative Perspectives on the Chemical Reaction Prediction Problem. *Int. J. Quantum Chem.* **2005**, *101* (5), 520–534. <https://doi.org/10.1002/qua.20307>.
- (13) Chattaraj, P. K. *Chemical Reactivity Theory: A Density Functional View*, CRC press.; Group, Taylor and Francis, Ed.; 2009. [https://doi.org/10.1007/978-3-642-61917-5\\_2](https://doi.org/10.1007/978-3-642-61917-5_2).
- (14) Roos, G.; Geerlings, P.; Messens, J. Enzymatic Catalysis: The Emerging Role of Conceptual Density Functional Theory. *J. Phys. Chem. B* **2009**, *113* (41), 13465–13475. <https://doi.org/10.1021/jp9034584>.
- (15) Orozco-Valencia, Á. U.; Vela, A. The Electrodonating and Electroaccepting Powers in Atoms. *J. Mex. Chem. Soc.* **2012**, *56* (3), 294–301. <https://doi.org/10.29356/jmcs.v56i3.293>.
- (16) Geerlings, P.; Chamorro, E.; Chattaraj, P. K.; De Proft, F.; Gázquez, J. L.; Liu, S.; Morell, C.; Toro-Labbé, A.; Vela, A.; Ayers, P. Conceptual Density Functional Theory: Status, Prospects, Issues. *Theor. Chem. Acc.* **2020**, *139* (2), 1–18. <https://doi.org/10.1007/s00214-020-2546-7>.
- (17) Chattaraj, P. K.; Roy, D. R. Update 1 of: Electrophilicity Index. *Chem. Rev.* **2007**, *107* (9), PR46–PR74. <https://doi.org/10.1021/cr078014b>.
- (18) Chattaraj, P. K.; Sarkar, U.; Roy, D. R. Electrophilicity Index. *Chem. Rev.* **2006**, *106* (6), 2065–2091. <https://doi.org/10.1021/cr040109f>.
- (19) Parr, R. G.; Yang, W. *Density Functional Theory of Atoms and Molecules*, Oxford uni.; New York, 1994.
- (20) Parr, R. G.; Donnelly, R. A.; Levy, M.; Palke, W. E. Electronegativity: The Density Functional Viewpoint. *J. Chem. Phys.* **1977**, *68* (8), 3801–3807. <https://doi.org/10.1063/1.436185>.
- (21) Parr, R. G.; Pearson, R. G. Absolute Hardness: Companion Parameter to Absolute Electronegativity. *J. Am. Chem. Soc.* **1983**, *105* (26), 7512–7516. <https://doi.org/10.1021/ja00364a005>.

- (22) Morell, C.; Grand, A.; Toro-Labbé, A. New Dual Descriptor for Chemical Reactivity. *J. Phys. Chem. A* **2005**, *109* (1), 205–212. <https://doi.org/10.1021/jp046577a>.
- (23) Morell, C.; Grand, A.; Toro-Labbé, A. Theoretical Support for Using the  $\Delta f(r)$  Descriptor. *Chem. Phys. Lett.* **2006**, *425* (4–6), 342–346. <https://doi.org/10.1016/j.cplett.2006.05.003>.
- (24) Yang, W.; Parr, R. G. Hardness, Softness, and the Fukui Function in the Electronic Theory of Metals and Catalysis. *Proc. Natl. Acad. Sci. U. S. A.* **1985**, *82* (20), 6723–6726. <https://doi.org/10.1073/pnas.82.20.6723>.
- (25) Shu-Bin, L. Conceptual Density Functional Theory and Some Recent Developments. *Acta Phys. -Chim. Sin* **2009**, *25* (3), 590–600.
- (26) Gázquez, J. L. Perspectives on the Density Functional Theory of Chemical Reactivity. *J. Mex. Chem. Soc.* **2008**, *52* (1), 3–10.
- (27) Geerlings, P.; De Proft, F.; Langenaeker, W. Conceptual Density Functional Theory. *Chem. Rev.* **2003**, *103* (5), 1793–1873. <https://doi.org/10.1021/cr990029p>.
- (28) Chermette, H. Chemical Reactivity Indexes in Density Functional Theory. *J. Comput. Chem.* **1999**, *20* (1), 129–154. [https://doi.org/10.1002/\(SICI\)1096-987X\(19990115\)20:1<129::AID-JCC13>3.0.CO;2-A](https://doi.org/10.1002/(SICI)1096-987X(19990115)20:1<129::AID-JCC13>3.0.CO;2-A).
- (29) Pearson, R. G. Absolute Electronegativity and Hardness: Application to Inorganic Chemistry. *Inorg. Chem* **1988**, *27*, 734–740.
- (30) Orozco-Valencia, A. U.; Gázquez, J. L.; Vela, A. Global and Local Partitioning of the Charge Transferred in the Parr-Pearson Model. *J. Phys. Chem. A* **2017**, *121* (20), 4019–4029. <https://doi.org/10.1021/acs.jpca.7b01765>.
- (31) Orozco-Valencia, A. U.; Gázquez, J. L.; Vela, A. Donation and Back-Donation Analyzed through a Charge Transfer Model Based on Density Functional Theory. *J. Mol. Model.* **2017**, *23* (7), 207.
- (32) Becke, A. D. Density-Functional Thermochemistry. III. The Role of Exact Exchange. *J. Chem. Phys.* **1993**, *98* (7), 5648–5652. <https://doi.org/10.1063/1.464913>.
- (33) Becke, A. D. Density-Functional Exchange-Energy Approximation with Correct Asymptotic Behavior. *Phys. Rev. A* **1988**, *38* (6), 3098–3100. <https://doi.org/10.1103/PhysRevA.38.3098>.
- (34) Lee, C.; Yang, W.; Parr, R. G. Into a Functional of the Electron Density F F. *Phys. Rev. B* **1988**, *37* (2), 785–789.
- (35) Krishnan, R.; Binkley, J. S.; Seeger, R.; Pople, J. A. Self-Consistent Molecular Orbital Methods. XX. A Basis Set for Correlated Wave Functions. *J. Chem. Phys.* **1980**, *72* (1), 650–654. <https://doi.org/10.1063/1.438955>.
- (36) McLean, A. D.; Chandler, G. S. Contracted Gaussian Basis Sets for Molecular Calculations. I. Second Row Atoms, Z=11-18. *J. Chem. Phys.* **1980**, *72* (10), 5639–5648. <https://doi.org/10.1063/1.438980>.
- (37) Latouche, C.; Skouteris, D.; Palazzetti, F.; Barone, V. TD-DFT Benchmark on Inorganic Pt(II) and Ir(III) Complexes. *J. Chem. Theory Comput.* **2015**, *11* (7), 3281–3289. <https://doi.org/10.1021/acs.jctc.5b00257>.
- (38) Stolaroff, A.; Rio, J.; Latouche, C. Accurate Computations to Simulate the Phosphorescence Spectra of Large Transition Complexes: Simulated Colors Match Experiment. *New J. Chem.* **2019**, *43* (30), 11903–11911. <https://doi.org/10.1039/c9nj02388g>.
- (39) Stolaroff, A.; Latouche, C. Accurate Ab Initio Calculations on Various PV-Based Materials: Which Functional to Be Used? *J. Phys. Chem. C* **2020**, *124* (16), 8467–8478. <https://doi.org/10.1021/acs.jpcc.9b10821>.
- (40) Miertus, S.; TOMASI, J. Approximate Evaluations of the the Electrostatic Free Energy and Internal Energy Changes in Solution Processes. **1982**, *65*, 239–245.
- (41) Miertus, S.; Scrocco, E.; Tomasi, J. Electrostatic Interaction of a Solute with a Continuum. A Direct Utilization of Ab Initio Molecular Potentials for the Prevision of Solvent Effects. **1981**, *55*, 117–129.
- (42) Frisch, M. J.; Trucks, G. W.; Schlegel, H. B.; Scuseria, G. E.; Robb, M. A.; Cheeseman, J. R. et al, Gaussian 09, Revision C.01, Gaussian, Inc., Wallingford CT 2009.
- (43) Gaussview Rev.3.09, Windows version, gaussian Inc., , Gaussian Inc., Pittsburgh. Pittsburgh 2003.

- (44) Allouche, A. R. Software News and Updates Gabedit — A Graphical User Interface for Computational Chemistry Softwares. *J. Comput. Chem.* **2011**, *32* (1), 174–182. <https://doi.org/10.1002/jcc>.
- (45) Glendening, E.D., Reed, A. E., Carpenter, J. E. and Weinhold, F., (2003) NBO Version 3.1. Gaussian Inc., 2003.
- (46) Johnson, P. A.; Bartolotti, L. J. P.; Ayers, W.; Fievez, T.; Geerlings., P. *Modern Charge Density Analysis*, Springer.; In: Gatti C., M. P., Ed.; In: C. Gatti, P. Macchi, New York, 2012.
- (47) Domingo, L. R.; Chamorro, E.; Pérez, P. Understanding the Reactivity of Captodative Ethylenes in Polar Cycloaddition Reactions. A Theoretical Study. *J. Org. Chem.* **2008**, *73* (12), 4615–4624. <https://doi.org/10.1021/jo800572a>.
- (48) Özcan, M.; Dehri, I.; Erbil, M. Organic Sulphur-Containing Compounds as Corrosion Inhibitors for Mild Steel in Acidic Media: Correlation between Inhibition Efficiency and Chemical Structure. *Appl. Surf. Sci.* **2004**, *236* (1–4), 155–164. <https://doi.org/10.1016/j.apsusc.2004.04.017>.
- (49) Scrocco, E.; Tomasi, J. *The Electrostatic Molecular Potential as a Tool for the Interpretation of Molecular Properties*, Springer.; Il, N. C., Ed.; Berlin/Heidelberg, 1973.
- (50) Sjoberg, P.; Politzer, P. Use of the Electrostatic Potential at the Molecular Surface to Interpret and Predict Nucleophilic Processes. *J. Phys. Chem.* **1990**, *94* (10), 3959–3961. <https://doi.org/10.1021/j100373a017>.
- (51) Murray, J. S.; Politzer, P. The Electrostatic Potential: An Overview. *Wiley Interdiscip. Rev. Comput. Mol. Sci.* **2011**, *1* (2), 153–163. <https://doi.org/10.1002/wcms.19>.
- (52) Gadre, S. R.; Suresh, C. H.; Mohan, N. Electrostatic Potential Topology for Probing Molecular Structure, Bonding and Reactivity. *Molecules* **2021**, *26* (11), 1–25. <https://doi.org/10.3390/molecules26113289>.
- (53) Berkowitz, M. Density Functional Approach to Frontier Controlled Reactions. *J. Am. Chem. Soc.* **1987**, *109* (16), 4823–4825. <https://doi.org/10.1021/ja00250a012>.
- (54) Martell, A. E.; Smith, R. .; Motekaitis, R. J. *NIST Critically Selected Stability Constants of Metal Complexes*; NIST, Ed.; NIST Gaithersburg, 2004.
- (55) Roy, D. R.; Parthasarathi, R.; Padmanabhan, J.; Sarkar, U.; Subramanian, V.; Chattaraj, P. K. Careful Scrutiny of the Philicity Concept. *J. Phys. Chem. A* **2006**, *110* (3), 1084–1093. <https://doi.org/10.1021/jp053641v>.